Chemistry, Physics and Technology of Surface. 2017. V. 8. N 4. P. 422-431

UDC 661.183.2:544.527.23 doi: 10.15407/hftp08.04.422

V.V. Sydorchuk, S.V. Khalameida, O.I. Poddubnaya, M.M. Tsyba, A.M. Puziy

CATION-CONTAINING ACTIVE CARBONS AS PHOTOCATALYSTS FOR DYES DEGRADATION

Institute for Sorption and Problems of Endoecology of National Academy of Sciences of Ukraine
13 General Naumov Str., Kyiv, 03164, Ukraine, E-mail: bilychi@ukr.net

We have oxidized commercial coconut-shell-based activated carbon Aquacarb 607C with nitric acid. Prepared oxidized active carbon has micro-mesoporous structure and contains surface carboxyl and phenol/enol groups. Cation-exchanged forms of active carbon were prepared via impregnation of oxidized active carbon with copper and cobalt salts in aqueous solutions. We studied photodegradation of rhodamine B, methyl orange, and phenol under UV- and visible irradiation using oxidized carbon as well as its Cu- and Co-containing forms as catalysts. Initial oxidized active carbon is photoactive toward rhodamine B and methyl orange under UV illumination but inactive under action of visible light. At the same time, cation-exchanged forms of active carbon has improved activity toward rhodamine B, methyl orange, and phenol under both UV- and visible irradiation. Cu-containing active carbon has maximal activity under UV-irradiation: the rate constant of rhodamine B photocatalytic degradation K_d is $2.9 \cdot 10^{-4}$ s^{-1} while Co-containing active carbon is the most active under visible irradiation – $K_d = 1.2 \cdot 10^{-4}$ s^{-1}. For 7 h irradiation, the degree of discoloration of dyes solutions reaches 90–95 % and degree of mineralization of dyes and phenol solutions (according to total organic carbon measurements) is 16–73 %.

Keywords: *active carbon, cation-exchanged forms, photocatalytic degradation, UV and visible irradiation, discoloration and mineralization*

INTRODUCTION

Active carbons (ACs) are high-porous materials with a huge specific surface area. Therefore, ACs are much more frequently used as a catalyst support than as a catalyst as well [1, 2]. Active carbons also are universal and effective adsorbents for removal organic and inorganic pollutants from gaseous and liquid media including water [3, 4]. Besides, oxidized ACs possess excellent cation-exchange properties [5, 6]. Photodegradation of organic pollutants using carbon materials as catalysts can be an alternative technique for water purification [7–9]. ACs possessing high specific surface area and adsorption capability can be perspective in photocatalytic processes, particularly as a support of photoactive species or constituent element in compositions with oxides [2, 7, 8, 10, 11]. However, the photocatalyst must be a semiconductive material with an electronic band structure which can generate electron–hole pairs after irradiation at a given wavelength (in the visible or UV region). Carbon materials show different electronic structure. Band gap E_g varies in a wide range: from the values characteristic for conductors to those for dielectrics [12]. Thus, diamond has E_g 5.5 eV [13], graphite is conductor while graphite oxide as well as graphene oxide are semiconductors with E_g 1.8–4.7 and 1.2–4.0 eV, respectively [14–16]. Therefore, these carbon oxides are active under UV- and visible irradiation [15, 17, 18].

Theoretical calculations and experimental measurements show that active carbons can have E_g within 4.8–2.9 eV depending on their origin, chemical composition, and mode of preparation [19–21]. These values allow activated carbons to be used as photocatalysts in UV- and visible region. The examples of ACs application without semiconductor additives for photocatalytic degradation of organic pollutants in aqueous media were reported [19, 21–23]. It has been shown that ACs are photocatalytically active under UV- and visible irradiation. S-doped carbon showed 2 times higher activity in photodegradation of methylene blue under visible and NIR irradiation as compared to that of commercial TiO_2. Gamma radiation treatment reduced the band gap values of the ACs and

increased sodium diatrizoate removal rate values under UV light. The presence of oxygen-containing groups on the surface is a necessary condition for photocatalytic activity of ACs. Nevertheless, the nature of photocatalytic activity of ACs and mechanism of initiation of oxidation reactions on carbon surface require further investigations.

In the present communication, the activity of oxidized AC and its cation-exchange forms in photodegradation of dyes and phenol under UV- and visible irradiation is studied.

EXPERIMENTAL

Materials. Commercial coconut-shell-based activated carbon Aquacarb 607C (Chemviron, Belgium) was oxidized with 20 % nitric acid for 5 h. After oxidation, carbon was extensively washed with hot water in Soxhlet extractor until neutral pH of wash waters and dried at 110 °C. Thus obtained, oxidized carbon was abbreviated as AC Ox-H. Copper and cobalt-doped carbons were prepared by impregnating 0.5 g of oxidized carbon AC Ox-H with 0.01 M solution of corresponding nitrates at pH 2.3 for copper and 2.6 for cobalt followed by washing with distilled water and drying. Therefore, cation-exchanged forms of AC (AC Ox-Cu and AC Ox-Co, respectively) were prepared.

Porous structure. Nitrogen adsorption isotherms were measured at -196 °C using an Autosorb-6 adsorption analyser (Quantachrome, USA). Pore size distributions (PSD) were calculated by Autosorb-1 software (Quantachrome, USA) using QSDFT method [24–26]. In calculation of PSD, a slit/cylindrical pore model was used. Specific surface area, S_{BET}, was calculated by BET method using nitrogen adsorption data in the relative pressure range chosen by recently proposed procedure [27]. The total pore volume, V_{tot}, was calculated by converting the amount of nitrogen adsorbed at a maximum relative pressure to the volume of liquid adsorbate. The micropore, V_{mi}, and mesopore, V_{me}, volumes were calculated from the cumulative pore size distribution as the volume of pores with sizes less than 2 nm and between 2 and 50 nm, respectively. The porous structure of cation-exchanged forms of AC is practically the same as that for initial oxidized AC.

Surface chemistry. Surface chemistry of oxidized carbon AC Ox-H was investigated by potentiometric titration method [28] performed in thermostatic vessel at 25 °C using a DL25 Titrator (Mettler-Toledo, Switzerland). The proton concentration was monitored using an LL pH glass electrode (Metrohm, Switzerland). The method is based on calculation of proton binding from raw potentiometric titration data followed by computation of proton affinity distribution using CONTIN method [29–31].

FTIR. The FTIR spectra in the range 4000–400 cm^{-1} for ACs were registered using a "Spectrum-One" spectrometer (Perkin-Elmer). The ratio of sample and KBr powders was 1:250.

Photocatalytic tests. Photocatalytic degradation under visible irradiation was performed in a glass reactor. LED Cool daylight lamp (Philips, 100 W) that has emission spectra exclusively in the visible range with broad maximum in the region 500–700 nm and local maximum around 440 nm was used as illumination source. UV-photocatalytic degradation is realized in quartz reactor using Hg lamp with emission maximum at 254 nm and power 30 W. The initial solution and ones after substrates degradation were analyzed spectrophotometrically (Lambda 35, Perkin Elmer Instruments) at λ_{max} = 553, 461 and 265 nm for rhodamine B (RhB), methyl orange (MO), and phenol (Ph), respectively, after centrifugation of reaction mixture (10 min at 8000 rpm). The concentration of their aqueous solutions was $1–3\cdot10^{-5}$ mol/l, $1–2\cdot10^{-5}$ mol/l, and 10 mg/l ($1.06\cdot10^{-4}$ mol/l), respectively. The calculation of photodegradation rate K_d (K_d^{UV} and K_d^{Vis} for reactions under UV- and visible illumination, respectively) was based on the temporal changes of substrates concentration after reaching the adsorption equilibrium (2 h). The obtained results are satisfactorily described by the first-order kinetic equation (correlation coefficient R^2 = 0.8–0.98). The control of pH value during photocatalytic reaction was performed using an apparatus pH-150M. The determination of total organic carbon (TOC) for selected solutions was measured with the help of a Shimazu TOC analyzer (model 5050A).

RESULTS AND DISCUSSION

Porous structure. Nitrogen adsorption-desorption isotherms for oxidized carbon AC Ox-H are shown in Fig. 1 *a*. The isotherm can be attributed to a combination of type I and type IVa of IUPAC classification [32]. A steep raise

of nitrogen uptake at very low p/p^0 is due to adsorption in narrow micropores with enhanced potential while gradual increase in nitrogen adsorption at medium and high relative pressures corresponds to monolayer-multilayer adsorption in mesopores followed by capillary condensation accompanied by small hysteresis of type H4. The isotherm is typical to micro-mesoporous carbons. Pore size distribution of oxidized carbon AC Ox-H (Fig. 1 *b*) shows narrow distribution of micropores with maximum at 1.1 nm and narrow distribution of mesopores with maximum at 2.2 nm. Oxidized carbon AC Ox-H shows high specific surface area of 1070 m^2/g with the total pore volume of 0.45 cm^3/g distributed mostly in micropores (82 %) and minor part in mesopores (18 %).

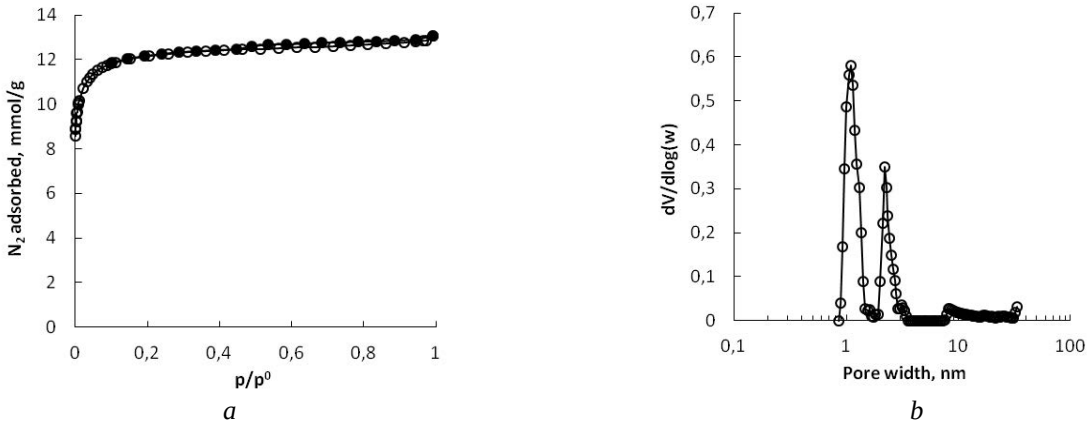

a *b*

Fig. 1. Nitrogen adsorption isotherm (*a*) and pore size distribution for oxidized carbon AC Ox-H (*b*)

Surface chemistry. Surface chemistry of oxidized carbon AC Ox-H was estimated by potentiometric titration method. Proton-binding isotherm for AC Ox-H is shown in Fig. 2 *a*. Proton binding by AC Ox-H decreases with increasing pH due to gradual dissociation of surface groups. The point of zero charge, where proton binding is zero, lies at 2.09 showing acidic character of the carbon. The shape of proton-binding isotherm for oxidized carbon AC Ox-H is characteristic for multifunctional cation exchangers containing surface groups of different acidity.

Proton affinity distribution of acid groups calculated by CONTIN method shows four peaks for AC Ox-H (Fig. 2 *b*). These peaks may be classed as strong carboxylic (0.13 mmol/g, pK 3.0), weak carboxylic (0.01 mmol/g, pK 5.3), and two types of phenolic and/or enol groups (0.06 mmol/g, pK 9.0; 1.32 mmol/g, pK 11.2). Total amount of surface groups equals to 1.52 mmol/g.

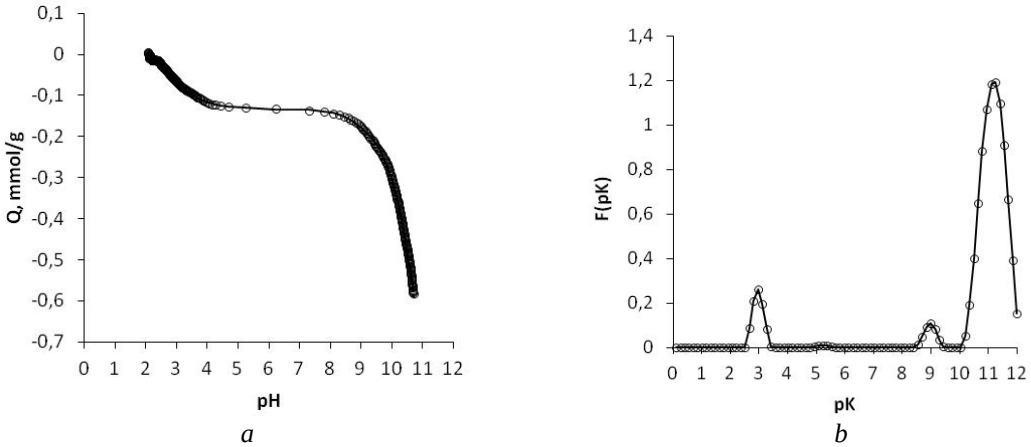

a *b*

Fig. 2. Proton-binding isotherm (*a*) and proton affinity distribution for oxidized carbon AC Ox-H (*b*)

Based on the concentration of strong carboxylic groups at carbon surface, the content of copper and cobalt in the cation-exchange forms can be about 0.76 and 0.82 % w/w, respectively.

Dose of carbon photocatalyst and substrate concentration. Since AC has high specific surface area and, consequently, high adsorption capacity, its content in reaction mixture is much less than that for oxide photocatalysts. For example, the authors of works [19, 21, 23] used content of AC within 0.05–0.2 g/l. For comparison, the content of 1–2 g/l is optimal for processes using TiO_2 as photocatalyst [33, 34]. We found out that adsorption of dyes by AC catalyst reaches 90–95 % when the content of AC is 0.15–0.2 g/l. In this case, the K_d is equal to $3–9\cdot10^{-4}$ s^{-1} when RhB is used. However, the measurement error in this case is large. Therefore, we used for all tested samples the content of AC equal to 0.1 g/l as optimal. Adsorption of dyes and phenol is 40–75 and 25–30 %, respectively, under these conditions. The difference in adsorption is obviously due to the fact that molecules of RhB and MO contain basic groups and phenol has only acidic group. So, phenol is less adsorbed on an acidic surface of AC. Indeed, the pH values are 6.9, 6.8 and 4.7 for initial solutions of RhB, MO and Ph, respectively, while the point of zero charge for AC equals 2.09 as mentioned above.

The influence of substrate concentration on photocatalytic activity of tested ACs samples was also studied. Thus, the dependence between RhB concentration and catalytic activity of AC Ox-Cu was found: K_d^{UV} value monotonically diminishes from 9.4 to $1.4\cdot10^{-4}$ s^{-1} when RhB concentration increases within $1–2\cdot10^{-5}$ mol/l. It should be noted that this is a well-known pattern for photocatalytic processes. All tested carbon catalysts become inactive at the RhB concentration $3.0\cdot10^{-5}$ mol/l. Obviously, this is due to the blocking of active surface sites by the adsorbed dye. As a result, the most suitable concentrations for photocatalytic testing were found: $1.8\cdot10^{-5}$, $2.0\cdot10^{-5}$, $1.06\cdot10^{-4}$ mol/l (10 mg/l) for RhB, MO and phenol, respectively.

Photocatalytic degradation of RhB. First, RhB was tested as substrate because the spectrum of its absorption is overlapped on a wide region with the emission spectrum of lamp – illumination source (the maxima are located at 553 and 565 nm, respectively). Therefore, the absorption of light and the excitation of dye molecules are possible.

It is necessary to note that initial oxidized AC predictably has no photocatalytic activity under visible illumination but exhibits noticeable activity under UV irradiation (Table). The photocatalytic properties of AC are improved after introduction of Cu^{2+} and Co^{2+} cations into its structure (Fig. 3, curves 2–4). (It's useful to show absorption/reflectance spectra of modified photocatalists if they are not absolutely black). Thus, K_d^{UV} value increases by one and a half times using AC Ox-Co sample (Table). The example of the changes in electron spectrum of RhB solution during its photodegradation under UV irradiation can be seen in Fig. 4. Under UV illumination, AC Ox-Cu sample showed somewhat less photocatalytic activity as compared to that of AC Ox-Co. On the contrary, AC Ox-Cu is more active under visible light (Table).

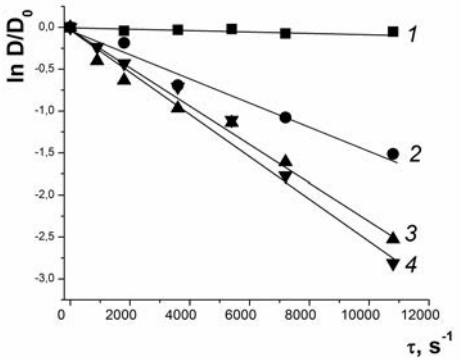

Fig. 3. Kinetic curves of RhB degradation for: AC Ox-H Vis (*1*), AC Ox-Cu Vis (*2*), AC Ox-Cu UV (*3*), AC Ox-Co UV (*4*)

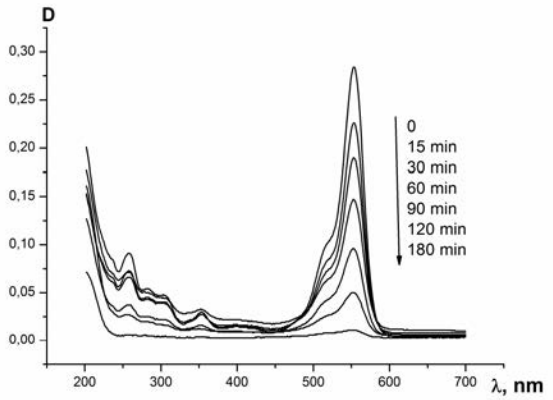

Fig. 4. The absorption spectra of solution of RhB after degradation under UV irradiation in the presence of AC Ox-Co

MO has maximum of absorption at 461 nm. So, its absorption spectrum slightly is overlapped with the emission spectrum of the used lamp. The character of the changes in the spectrum during the degradation of MO is shown in Fig. 5 *a*: monotonic decrease of band at 461 nm is observed with an increase in the duration of UV irradiation. Besides, a slight blue shift of the absorption maximum (up to 545–542 nm) is seen after 6–8 h illumination. The kinetic curve of this process is presented in Fig. 6 (curve 2). Similar spectra and kinetic curve were obtained for the photocatalytic degradation of phenol (Fig. 5 *b* and Fig. 6, curve 1, respectively). In should be noted that maximum of absorption for phenol is in the UV region – at 265 nm.

Table. The values of rate constant degradation at optimal concentration of substrates

No	Photocatalyst	Substrate	$K_d^{UV}\cdot10^4$, s^{-1}	$K_d^{Vis}\cdot10^4$, s^{-1}
1	AC Ox-H	RhB	1.8	inactive
2	AC Ox-Cu	RhB	2.2	1.2
3	AC Ox-Co	RhB	2.9	0.5
4	AC Ox-H	MO	0.1	inactive
5	AC Ox-Cu	MO	0.3	0.6
6	AC Ox-Co	MO	0.6	0.5
7	AC Ox-H	Phenol	inactive	inactive
8	AC Ox-Cu	Phenol	0.15	0.1
9	AC Ox-Co	Phenol	0.24	0.1

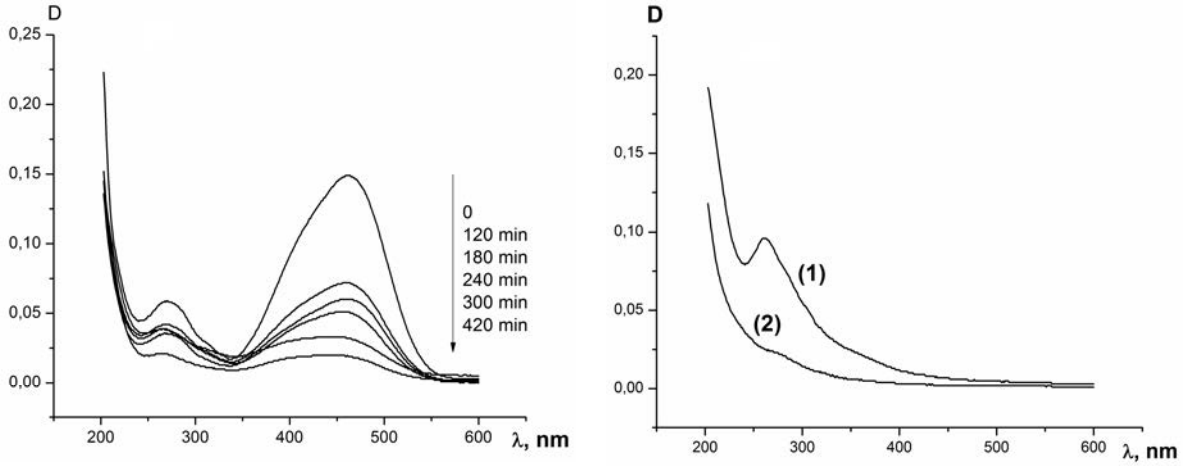

a *b*

Fig. 5. The absorption spectra of MO solution after degradation under UV irradiation in the presence of AC Ox-Co (*a*), phenol solution after adsorption (*1*) and degradation for 420 min (*2*) under UV irradiation in the presence of AC Ox-Co (*b*)

The rate constant of degradation values calculated for these processes as well as for visible photocatalytic degradation are also presented in Table.

Discussion. It can be seen from the data of spectrophotometric measurements that photocatalytic processes using Cu- and Co-containing ACs result in degradation of substrates under both UV- and visible illumination. Initial oxidized AC showed activity toward the RhB and MO only under the action of UV light.

The optical density of substrate solutions after illumination (D) compared with that for solutions after adsorption (D_0) reduces 4–12 times for 7 h. Therefore, the degree of discoloration reaches 90–95 % for catalysts with highest activity. At the same time, decreasing in TOC value is measure of pollutants total mineralization [35]. In our case, TOC is within

16–73 %. Moreover, the FTIR spectra registered for AC Ox-Cu catalyst (Fig. 7) indicate a possibility of degradation of adsorbed RhB. Their comparison shows that spectrum after RhB adsorption (Fig. 7, curve 2) contains broad poorly resolved absorption bands (a.b.) in the region (950–1350 cm^{-1}) where there are a.b. characteristic for RhB (Fig. 7, curve 1). At the same time, these a.b. are absent in the spectrum obtained for the same sample after photocatalysis (Fig. 7, curve 3).

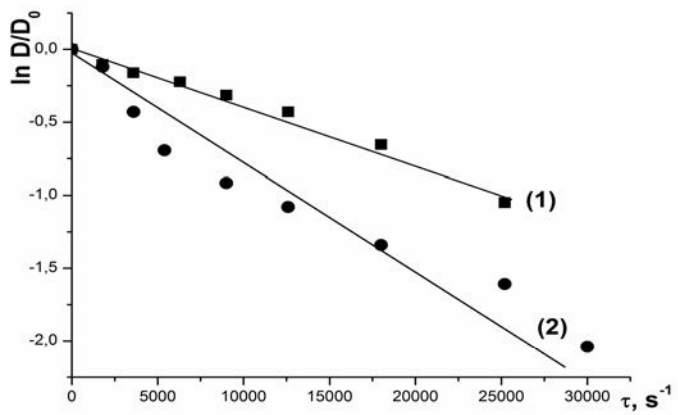

Fig. 6. The kinetic curves of photocatalytic degradation of phenol (*1*) and methyl orange (*2*) under UV illumination using AC Ox-Co as catalyst

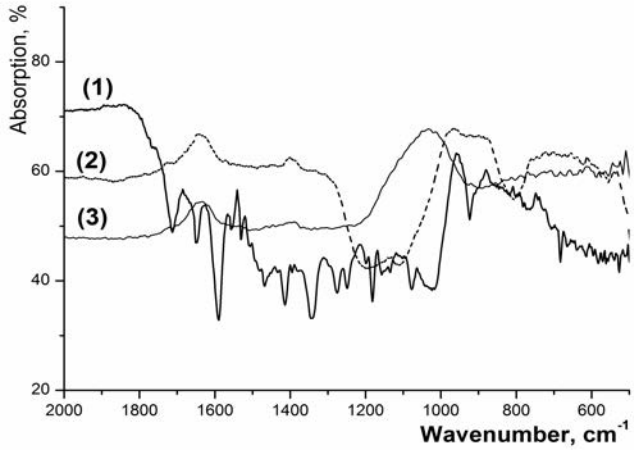

Fig. 7. FTIR spectra for initial RhB (*1*), AC Ox-Cu catalyst with adsorbed RhB (*2*) and the same after phocatalysis (*3*)

Maximal rate of degradation is observed for rhodamine B. This may be due to the fact that RhB molecules absorb light photons and their excitation is possible [35, 36]. On the other hand, it is well known that photocatalytic degradation of RhB can occur by two pathways [36, 37]: as de-ethylation process in a stepwise manner (with the formation of the three intermediates from RhB to completely de-ethylated Rh110) or as a direct cleavage of the chromophore rings. The gradual blue shift in λ_{max} of the spectrum of RhB is observed in the first case and the reduction in the absorbance without shift takes place in the second case. As can be seen from Fig. 4, the RhB degradation in the presence AC photocatalyst occurs in accordance with the second mechanism: only decrease in the intensity of band at 553 nm is observed. Simultaneously, reduction of insensity of band in UV region, namely around 260 nm, takes place (Fig. 4). The latter indicates the destruction of benzene rings in the dye molecules [38]. The same results were obtained using all tested photocatalysts under UV and visible illumination. The similar

findings were described for degradation of rhodamine B and safranin T using vanadium and molybdenum oxides as photocatalysts [39].

It is known that the mechanism of initiation of photocatalytic reaction under UV and visible light illumination can be different: *via* absorbing irradiation by photocatalysts or substrate molecules (photosensitization process) [35, 40]. Based on the literature data on semiconductor properties of oxidized carbons [19–21], it can be predicted that due to the action of UV, and possibly visible irradiation, the pairs of electron-hole is generated on the surface. Formed electrons are promoted from the valence band to the conduction one. As a result of this, photoactive species (likely OH* radicals) are generated which initiate the processes of substrate oxidation. UV degradation of RhB, MO and Ph using initial as well as Cu- and Co-containing ACs obviously occurs according to this mechanism.

In addition, the comparison of the emission spectrum for used lamp of visible light with absorption spectra for RhB and MO indicates that a significant portion of the irradiation can be absorbed by dye molecules. For these substrates, the primary act of photocatalysis may also be excitation of dye molecules and therefore a photosensitization mechanism can be realized. Phenol absorbs only in the UV region. So, in case of phenol, obviously, only the first mechanism is realized, namely formation of electron-hole pairs.

The activity of AC Ox-Cu and AC Ox-Co catalysts under visible illumination can be associated with formation of additional levels in band gap of carbon as it occurs due to the doping of oxides with metals [35,41] or narrowing of band gap. The latter was observed by authors of work [19, 21] as a result of introduction of heteroatoms and defects into carbon structure.

An alternative mechanism of photocatalytic oxidation process initiation can be connected with superoxide ion $O_2^{\bullet -}$ which is formed at the surface of AC in contact with aqueous solution containing dissolved oxygen. Superoxide ion take an important part in oxidation reactions *via* interaction with adsorbed molecules of substrates [20, 42–44].

CONCLUSIONS

Initial oxidizing active carbon has micro-mesoporous structure with predominance of micropores and contains four types of surface acidic groups. Cu- and Co- containing ACs were prepared *via* cation exchange process with the participation of surface carboxylic groups. Initial AC is photocatalitically active toward dyes (RhB and MO) under UV illumination but inactive in visible region. Cationic forms of AC as doped semiconductor oxides have improved photocalytic activity in the process of degradation of dyes and phenol under UV and visible irradiation. The degradation is accompanied by partial mineralization of substrates. The practical significance of the results obtained is that carbon adsorbents with sorbed cations, instead of regeneration, can be reused in processes of photocatalytic degradation of pollutants in aqueous media.

Катіон-вмісне активоване вугілля як фотокаталізатори деградації барвників

В.В. Сидорчук, С.В. Халамейда, О.І. Піддубна, М.М. Циба, О.М. Пузій

Інститут сорбції та проблем ендоекології Національної академії наук України
вул. Генерала Наумова, 13, Київ, 03164, Україна, bilychi@ukr.net

Окиснене вугілля та його катіонообмінні форми використані як фотокаталізатори в процесах деградації барвників (родамін Б, метилоранж) та фенолу під дією УФ та видимого світла. Встановлено, що вихідне окиснене вугілля є активним в умовах УФ опромінення, але неактивне у видимій області. Введення в активоване вугілля добавок міді та кобальту сприяє значному збільшенню фотокаталітичної активності отриманих каталізаторів. Мідь-вмісне вугілля є найактивнішим в УФ області, а кобальт-вмісне – у видимій області. Ступінь знебарвлення розчинів барвників досягає 90–95 %, а ступінь їх мінералізації складає 16–73 %.

Ключові слова: *активоване вугілля, катіонообмінні форми, фотокаталітична деградація, УФ- та видиме випромінювання, знебарвлення та мінералізація*

Катион-содержащие активированные угли как фотокатализаторы деградации красителей

В.В. Сидорчук, С.В. Халамейда, О.И. Поддубная, Н.Н. Цыба, А.М. Пузий

Институт сорбции и проблем эндоэкологии Национальной академии наук Украины
ул. Генерала Наумова, 13, Киев, 03164, Украина, bilychi@ukr.net

Окисленный уголь и его катионобменные формы использованы как фотокатализаторы в процессах деградации красителей (родамин Б, метилоранж) и фенола под действием УФ и видимого облучения. Установлено, что исходный окисленный уголь является активным в условиях УФ облучения, но неактивным в видимой области. Введение в активированный уголь добавок меди и кобальта способствует значительному увеличению фотокаталитической активности полученных катализаторов. Медь-содержащий уголь является наиболее активным в УФ области, а кобальт-содержащий уголь – в видимой области. Степень обесцвечивания растворов красителей достигает 90–95 %, а степень их минерализации – 16–73 %.

Ключевые слова: *активированные угли, катион-обменные формы, фотокаталитическая деградация, УФ и видимое облучение, обесцвечивание и минерализация*

REFERENCES

1. Rodriguez-Reinoso F. The role of carbon materials in heterogeneous catalysis. *Carbon*. 1998. **36**(3): 159.
2. Trogadas P., Fuller T.F., Strasser P. Carbon as catalyst and support for electrochemical energy conversion. *Carbon*. 2014. **75**: 5.
3. Moreno-Castilla C. Adsorption of organic molecules from aqueous solutions on carbon materials. *Carbon.* 2004. **42**(1): 83.

4. Radovic L.R., Moreno-Castilla C., Rivera-Utrilla J. Carbon materials as adsorbents in aqueous solutions. *Chemistry and Physics of Carbon*. V. 27. (New York: Marcel Dekker, Inc., 2000).
5. Tarkovskaya I.A. *Oxidized carbon*. (Kiev: Naukova dumka, 1981). [in Russian].
6. Moreno-Castilla C., Alvarez-Merino M.A., López-Ramón M.V., Rivera-Utrilla J. Cadmium ion adsorption on different carbon adsorbents from aqueous solutions. Effect of surface chemistry, pore texture, ionic strength, and dissolved natural organic matter. *Langmuir*. 2004. **20**(19): 8142.
7. Bagheri S., Julkapli N.M., Abd Hamid S.B. Functionalized activated carbon derived from biomass for photocatalysis applications perspective. *Int. J. Photoenergy*. 2015. **2015**: Article ID 218743.
8. Wang J., Ng Y.H., Lim Y.-F., Ho G.W. Vegetable-extracted carbon dots and their nanocomposites for enhanced photocatalytic H_2 production. *RSC Adv*. 2014. **4**(83): 44117.
9. Lu S., Panchapakesan B. Photoconductivity in single wall carbon nanotube sheets. *Nanotechnology*. 2006. **17**(8): 1843.
10. Haro M., Velasco L.F., Ania C.O. Carbon-mediated photoinduced reactions as a key factor in the photocatalytic performance of C/TiO_2. *Catal. Sci. Technol*. 2012. **2**(11): 2264.
11. An G., Ma W., Sun Z., Liu Z., Han B., Miao S., Miao, Z., Ding, K. Preparation of titania/carbon nanotube composites using supercritical ethanol and their photocatalytic activity. *Carbon*. 2009. **45**(9): 1795.
12. Oh Y.J., Kim S., Lee I.H., Lee J., Chang K.J. Direct band gap carbon superlattices with efficient optical transition. *Phys. Rev. B*. 2016. **93**(8): 1.
13. Klimm D. Electronic materials with a wide band gap: recent developments. *Int. Union Crystallogr. J.* 2014. **1**(Pt 5): 281.
14. Jeong H.K., Yang C., Kim B. S., Kim Ki-J. Valence band of graphite oxide. *Europhys. Lett.* 2010. **92**(3): 37005.
15. Bustos-Ramírez K., Barrera-Díaz C.E., Icaza-Herrera M.De., Martínez-Hernández A.L., Natividad-Rangel R., Velasco-Santo C. 4-chlorophenol removal from water using graphite and graphene oxides as photocatalysts. *J. Environ. Health. Sci. Eng*. 2015. **13**: 33.
16. Velasco-Soto M.A., Pérez-García S.A., Alvarez-Quintana J., Cao Y., Nyborg L., Licea-Jiménez L. Selective band gap manipulation of graphene oxide by its reduction with mild reagents. *Carbon*. 2015. **93**: 967.
17. Yeh Te-Fu, Syu J.-M., Cheng C., Chang T.-H., Teng H. Graphite Oxide as a Photocatalyst for Hydrogen Production from Water. *Adv. Funct. Mater*. 2010. **20**(14): 2255.
18. Xiang Q., Yu J., Jaroniec M. Graphene-based semiconductor photocatalysts. *Chem. Soc. Rev*. 2012. **41**(2): 782.
19. Bandosz T.J., Matos J., Seredych M., Islam M.S.Z., Alfano R. Photoactivity of S-doped nanoporous activated carbons: A new perspective for harvesting solar energy on carbon-based semiconductors. *Appl. Catal. A*. 2012. **445–446**: 159.
20. Strelko V.V., Kartel N.T., Dukhno I.N., Kuts V.S., Clarkson R.B., Odintsov B.M. Mechanism of reductive oxygen adsorption on active carbons with various surface chemistry. *Surf. Sci*. 2004. **548**(1–3): 281.
21. Velo-Gala I., López-Peñalver J.J., Sánchez-Polo M., Rivera-Utrilla J. Activated carbon as photocatalyst of reactions in aqueous phase. *Appl. Catal. B.* 2013. **142–143**: 694.
22. Velasco L.F., Fonseca I.M., Parra J.B., Lima J.C., Ania C.O. Photochemical behaviour of activated carbons under UV irradiation. *Carbon*. 2012. **50**(1): 249.
23. Velasco L.F., Maurino V., Laurenti E., Fonseca I.M., Lima J.C., Ania C.O. Photoinduced reactions occurring on activated carbons. A combined photooxidation and ESR study. *Appl. Catal. A*. 2013. **452**: 1.
24. Gor G.Y., Thommes M., Cychosz K.A., Neimark A.V. Quenched solid density functional theory method for characterization of mesoporous carbons by nitrogen adsorption. *Carbon*. 2012. **50**(4): 1583.
25. Landers J., Gor G.Y., Neimark A.V. Density functional theory methods for characterization of porous materials. *Colloids Surf. A.* 2013. **437**: 3.
26. Neimark A.V., Lin Y., Ravikovitch P.I., Thommes M. Quenched solid density functional theory and pore size analysis of micro-mesoporous carbons. *Carbon*. 2009. **47**(7): 1617.

27. Rouquerol J., Llewellyn P., Rouquerol F. Is the BET equation applicable to microporous adsorbents? In: *COPS-7: Characterization of Porous Solids VII*. V. 160. (Amsterdam: Elsevier, Studies in Surface Science and Catalysis, 2007).
28. Lützenkirchen J., Preočanin T., Kovačević D., Tomišić V., Lövgren L., Kallay N. Potentiometric titrations as a tool for surface charge determination. *Croat. Chem. Acta*. 2012. **85**(4): 391.
29. Puziy A.M., Poddubnaya O.I., Ritter J.A., Ebner A.D., Holland C.E. Elucidation of the ion binding mechanism in heterogeneous carbon-composite adsorbents. *Carbon*. 2001. **39**(15): 2313.
30. Puziy A.M., Kochkin Y.N., Poddubnaya O.I., Tsyba M.M. Ethyl tert-butyl ether synthesis using carbon catalysts from lignocellulose. *Adsorpt. Sci. Technol.* 2017. **35**(5–6): 473.
31. Myglovets M., Poddubnaya O.I., Sevastyanova O., Lindström M.E., Gawdzik B., Sobiesiak M., Tsyba M.M., Sapsay V.I., Klymchuk D.O., Puziy A.M. Preparation of carbon adsorbents from lignosulfonate by phosphoric acid activation for the adsorption of metal ions. *Carbon*. 2014. **80**: 771.
32. Thommes M., Kaneko K., Neimark A.V., Olivier J.P., Rodriguez-Reinoso F., Rouquerol J., Sing K.S.W. Physisorption of gases, with special reference to the evaluation of surface area and pore size distribution (IUPAC Technical Report). *Pure Appl. Chem.* 2015. **87**(9–10): 1051.
33. Kapinus E., Viktorova T., Khalyavka T. Dependence of the rate of photocatalytic decomposition of safranine on the catalyst concentration. *Theor. Exp. Chem.* 2009. **45**(2): 114.
34. Gupta V.K., Jain R., Mittal A., Mathur M., Sikarwar S. Photochemical degradation of the hazardous dye Safranin-T using TiO_2 catalyst. *J. Colloid Interface Sci*. 2007. **309**(2): 464.
35. Rauf M.A., Ashraf S.S. Fundamental principles and application of heterogeneous photocatalytic degradation of dyes in solution. *Chem. Eng. J.* 2009. **151**(1–3): 10.
36. Zhu Z.F., Zhou J.Q., Wang X.F., He Z.L., Liu H. Effect of pH on photocatalytic activity of SnO_2 microspheres via microwave solvothermal route. *Mater. Res. Innovations.* 2014. **18**(1): 8.
37. Sangami G., Dharmaraj N. UV–visible spectroscopic estimation of photodegradation of rhodamine-B dye using tin(IV) oxide nanoparticles. *Spectrochim. Acta A Mol. Biomol. Spectrosc.* 2012. **97**: 847.
38. Merka O., Yarovyi V., Bahnemann D.W., Wark M. pH-control of the photocatalytic degradation mechanism of Rhodamine B over $Pb_3Nb_4O_{13}$. *J. Phys. Chem. C.* 2011. **115**(16): 8014.
39. Sydorchuk V.V., Khalameida S.V., Zazhigalov V.O., Khanina O.A. Photocatalytic degradation of dyes in the presence of mechanochemically modified vanadium and molybdenum oxides. *Him. Fiz. Tehnol. Poverhni*. 2013. **4**(3): 266. [in Ukrainian].
40. Wu T., Liu G., Zhao J. Photoassisted degradation of dye pollutants. V. Self-photosensitized oxidative transformation of Rhodamine B under visible light irradiation in aqueous TiO_2 dispersions. *J. Phys. Chem. B.* 1998. **102**(30): 5845.
41. Khalameida S., Samsonenko M., Sydorchuk V., Starchevskyy V., Zakutevskyy O., Khyzhun O. Synthesis, physical-chemical properties of tin dioxide doped with chromium(III), silver, zinc compounds and photodegradation of some substrates with its use under visible light. *Theor. Exp. Chem.* 2017. **53**(1): 40.
42. Matzner S., Boehm H.P. Influence of nitrogen doping on the adsorption and reduction of nitric oxide by activated carbons. *Carbon*.1998. **36**(11): 1697.
43. Strelko V.V., Kutz V.S., Thrower P.A. On the mechanism of possible influence of heteroatoms of nitrogen, boron and phosphorus in a carbon matrix on the catalytic activity of carbons in electron transfer reactions. *Carbon*. 2000. **38**(10): 1453.
44. Hayyan M., Hashim M.A., Alnashef I.M. Superoxide ion: generation and chemical implications. *Chem. Rev.* 2016. **116**(5): 3029.

Received 13.07.2017, accepted 30.10.2017